Networks and Heterogeneous Media

https://www.aimspress.com/journal/nhm

NHM, 20(1): 89–103.
DOI: 10.3934/nhm.2025006
Received: 08 October 2024
Revised: 23 December 2024
Accepted: 25 December 2024
Published: 22 January 2025

Research article

The shifted wavelet (q, q')-entropy and the classification of stationary fractal signals

Julio César Ramírez Pacheco[1,*], Joel Antonio Trejo-Sánchez[2] and Luis Rizo-Domínguez[3]

[1] Cancun Multidisciplinary Sciences Division, Autonomous University of Quintana Roo, UQRoo, 77519, Cancun, Quintana Roo, Mexico

[2] SECIHTI - Center for Research in Mathematics

[3] Department of Electronics, Systems and Informatics, ITESO, Western Institute of Technology and Higher Education, Guadalajara, Mexico

* **Correspondence:** Email: juliocr@uqroo.edu.mx.

Abstract: In this article, a wavelet entropy, which behaves as a shifted version of the standard wavelet (q, q')-entropy of fractal signals, is presented. The shifted wavelet (q, q')-entropy is obtained by computing the standard (q, q')-entropy functional on a weighted relative-wavelet-energy (RWE) representation of fractal signals; it is shown that the weight within the RWE plays the role of a shifting factor in the characteristics of the standard wavelet (q, q')-entropy. Therefore the shifted wavelet (q, q')-entropy relocates the wavelet entropy values to any point of the fractality index range, which allows us to analyze a wide variety of fractal signal families thus improving on previously proposed entropies in the literature. Information planes for these entropies are obtained using different shifts and values of parameters q and q', which allow us to highlight the potential applications for a fractal signal analysis. Moreover, an experimental study using synthesized exact fractal signals shows that the shifted wavelet entropy can classify stationary long-memory signals from short-memory ones and can also be used to differentiate other fractal signal families.

Keywords: fractals; fractal analysis; entropy; wavelet entropy; fractal signal classification

1. Introduction

In the beginning, fractal analyses were applied in precipitation patterns in hidrology [1] and foreign exchange rates in economy [2]. However, in recent years, fractality is an important concept in fields such as Physiology [3], Economics [4], Finance [5], Chemistry [6] and Dentistry [7], to name but a few. For instance, in Physiology, fractal analyses have been applied in heart-beat dynamics [8,9], stride-to-stride duration [10] and human gaze dynamics [11], where the fractality index allows researchers

to distinguish amongst healthy and diseased people [12]. This makes fractal analyses essential in Physiology since it can be used as a biomarker to highlight some affections early [13, 14]. Moreover, fractals are present in plasma turbulence in Physics [15, 16] and variable-bit-rate (VBR) video traffic in computer networks [17], where it can be used to enhance the performance and design of network algorithmics.

In all the above applications, the fractality index (popularly known to as the Hurst index) plays a prominent role an indicator of the "state" of a phenomena; therefore, their efficient estimation is crucial in any fractal signal analysis framework [18]. Many estimators of the fractality parameter or Hurst-index have been proposed in the literature; for instance, the wavelet method [19, 20] and the detrended fluctuation analysis (DFA) [21] are two popular estimators that are used across disciplines [22–24]. For an in-depth presentation of some definitions and algorithms to estimate the fractality exponent, the interested reader may refer to [18, 25–28]. Fractal stochastic models, fractal signal estimation, fractal signal analysis and the more recent fractal signal classification are common terms associated with fractality. In principle, fractal signal classification is defined as the process of determining the stationary or nonstationary nature of any fractal [29, 30]; nowadays, it defines the process of determining wheter or not a given fractal lies within a fractality interval, α_T. Naturally, this fractal signal classification term may be extended to other intervals; however, the above definition is broader than the original stationary/nonstationary one. Historically, the importance of the fractal signal classification stems from the fact that it determines characteristics such as the type of Hurst-index estimator to be used, the form of autocorrelations, and the smoothness of sample paths.

Many techniques for fractal signal classification (in the stationary/nonstationary sense) have been proposed in the literature, such as the signal summation conversion (SSC) [30, 31] and various techniques based on wavelet entropies [32, 33]. It is important to note that no methodology exists in the literature to classify fractal signals within a more general fractality range.

Motivated by the latter, in this article, a new class of wavelet entropy that shifts its behavior is proposed and its application for fractal signal classification is briefly studied. In a more general sense, entropies allow researchers to quantify the information content or complexity of a random signal or system [34, 35]. Entropies can be categorized as extensive, such as the Shannon entropy, or nonextensive, such as the Tsallis [36] and Abe entropies [37]. Nonextensive entropies have proven to be useful in applications, where long-range interactions, long-range correlations, and fractality are present. Now, entropic quantifiers are widely used in the literature and generalizations have been proposed in order to deal with the ever increasing complexity of the data under study. Generalizations may be achieved by changing the domain of definition of the signal, such as in spectral [38] and wavelet entropies [39, 40], or by adding extra parameters to increase the flexibility and the posibility to switch the extensive/nonextensive entropy character, such as in the (q, q')-entropy [41].

Wavelet entropies are already in use in numerous applications such as structural damage identification in vibration signals [42] and detecting weak level-shifts added to synthesized fractal signals [43]. In this article, a wavelet entropy that behaves as a shifted version of the wavelet (q, q')-entropy [44] is proposed. The shift in the characteristics of the wavelet (q, q')-entropy is achieved by computing the entropy in a weighted relative-wavelet-energy (RWE) representation of the fractal signal; it is shown that the weight and the shift within the resulting entropy are related. A closed-form expression for the shifted wavelet (q, q')-entropy is obtained along with their information planes and potential applications. Additionally, an experimental study is presented, where it is shown

that the shifted wavelet (q, q')-entropy allows for the classification of stationary long-memory from short-memory fractals, which is a feature not available in current fractal signal classification schemes.

The rest of the article is organized as follows. In Section 2, a review of the theory of fractals, their wavelet analysis, and a brief description of the wavelet (q, q')-entropy is presented. Moreover, the weighted RWE is defined and the shifted wavelet (q, q')-entropy computed. The shifted wavelet (q, q') information planes are derived in Section 3; based on these, important applications for fractals are highlighted. Furthermore, Section 4 presents a brief but complete application of the proposed shifted wavelet (q, q')-entropy for the classification of only long-memory/short-memory and to discriminate long-memory signals. Finally, Section 5 concludes the paper.

2. Materials and methods

2.1. A review of fractals, wavelets and the wavelet analysis of fractal signals

Fractality is defined in a variety of ways; however, the most popular definition is based on the behavior of their power spectral density (PSD). In this context, a random signal, X_t, is called fractal if their PSD, $S_{X_t}(f)$, behaves as a power-law in a range of frequencies, i.e., as in the following equation:

$$S_{X_t}(f) \sim c_f |f|^{-\alpha}, \quad f \in (f_a, f_b), \tag{2.1}$$

where c_f is a constant, $\alpha \in \mathbb{R}$ is the fractality parameter, and f_a, f_b represent the lower and upper power-law bounds respectively [19]. Depending upon α, f_a, and f_b, several well-known fractal random processes are obtained (e.g., when $f_b > f_a$, $f_a \to 0$ and $0 < \alpha < 1$, long-memory signals result). Moreover, for all $\alpha \in \mathbb{R}$ the signals are self-similar in the sense that their distributional properties are invariant under dilations in time and space [45] ($X(at) = a^H x(t)$). Stationarity and nonstationarity are two characteristics of fractal signals: the former is found when $\alpha < 1$ and the latter when $\alpha > 1$ [18]. In addition, long-memory stationary signals appear when $0 < \alpha < 1$ and short-memory stationary signals when $-1 < \alpha < 0$. Moreover, when $\alpha \in (1, 3)$, the signal is regarded as a fractal motion (fractional Brownian motion, fBm), and when $\alpha \in (3, 5)$, it is called an extended fractional motion [25,46]. Fractal motions are processes whose autocovariance (ACV) function is given by the following:

$$\mathbb{E}B_H(t)B_H(s) = \frac{\sigma^2}{2}\left\{|t|^{2H} + |s|^{2H} - |t-s|^{2H}\right\}, \tag{2.2}$$

and their corresponding PSD as $f \to 0$ is as follows:

$$S_{fBm}(f) \sim c|f|^{-(2H+1)}, \tag{2.3}$$

where $H \in (0, 1)$. According to Eq (2.1), fBm is a fractal signal with $\alpha = 2H + 1$ [18, 25]. The parameter H is commonly called "the Hurst" exponent in honor of English hidrologist Harold Edwin Hurst. Fractional Gaussian noise (fGn), which is obtained from a fBm process via a differencing operation, is stationary, self-similar, Gaussian, and has a PSD of the following form [18, 25, 26, 47]:

$$S_{fGn} = 4\sigma_X^2 c_H \sin^2(\pi f) \sum_{j=-\infty}^{\infty} \frac{1}{|f + j|^{2H+1}}, \quad |f| < \frac{1}{2}, \tag{2.4}$$

for $H \in (0,1)$. In the limit of $f \to 0$, the PSD of fGn behaves as $S_{fGn} \sim c|f|^{-2H+1}$ and therefore is a fractal signal with $\alpha = 2H - 1$. Several other processes are also fractal since their PSD resembles the form given in Eq (2.1) (e.g., the fractional auto-regressive integrated moving-average (f-ARIMA) process [48,49] and the so-called pure-power-law (PPL) process described in the work of Percival [50]). Literature on fractals have proposed analyses, simulation, and estimation frameworks based on time, frequency, and time-scale domains. More recently, wavelet information tools have been proposed to unveil the properties of fractal signals. This article proposes a generalization of the wavelet (q, q')-entropy by further averaging the RWE with dyadic weights, which has the effect of relocating (within the fractality index range) the entropies of fractal signals. Wavelet analysis have found applications in a variety of fields of science due to its versatility for representing and analyzing deterministic and random signals [51, 52]. They are particularly appropriate for nonstationary signals and may conveniently represent a signal in terms of a discrete sum of wavelets (discrete wavelet transform (DWT)) or by a continuous sum of ones (continuous wavelet transform (CWT)). In the context of fractal signals, wavelet analyses have found extensive applicability [20,53,54], and based on the multiresolution signal decomposition [55] given by,

$$X_t = \sum_{j=1}^{L} \sum_{k=-\infty}^{\infty} d_x(j,k)\psi_{j,k}(t), \tag{2.5}$$

where $d_X(j,k)$ is the DWT of X_t and $\{\psi_{j,k}(t) = 2^{-j}\psi_o(2^{-j}t - k),\ j,k \in \mathbb{Z}\}$, permits us to quantify contributions of each scale in the characteristics of the signal. Since $d_X(j,k)$ represents a random process for each j, [56] many statistical quantities may be computed based on it such as means, cumulants, and entropies. A statistical measure of particular importance is the wavelet spectrum, which is given by the following relation:

$$\mathbb{E}d_X^2(j,k) = \int_{-\infty}^{\infty} S_X(2^{-j}f)|\Psi(f)|^2\, df, \tag{2.6}$$

where $\Psi(f)$ represents the Fourier integral of the mother wavelet $\psi_0(t)$ and $S_X(.)$ is the process' PSD. For fractal processes, the wavelet spectrum takes the following form [20]:

$$\mathbb{E}d_X^2(j,k) \sim 2^{j\alpha} \times C, \tag{2.7}$$

where C is a constant that depends on the fractal process under analysis, and α is the fractality parameter. The wavelet spectrum given in Eq (2.7) plays a fundamental role in the entropic quantities that will be presented in the paper.

2.2. The time and wavelet (q, q')-entropy

As mentioned earlier, entropic functionals have found widespread applications in many fields of science for the analysis of complex signals [57, 58]. The standard Shannon entropy has proven to be useful; however, in some applications, more robust entropic functionals are needed. Nonextensive entropies are those such robust measures which generalize the Shannon entropy and allow researchers to study phenomena with long-range forces, long-memory, power-laws, and systems with asymptotic long-tails [41,59]. In addition, many of these entropies provide researchers with additional parameters

to fine-tune analyses. Many entropic functionals may be represented by the following form:

$$\mathcal{S} = -\sum_i p_i \Delta(p_i),\ (i = 1, 2 \ldots N), \tag{2.8}$$

and differ by the form adopted by $\Delta(p_i)$. For instance, Tsallis entropy has $\Delta(p_i) = (p_i^{1-q} - 1)/(1-q)$, the κ-entropy [60] has $\Delta(p_i) = (p_i^{\kappa} - p_i^{-\kappa})$, and the Abe entropy [61] has $\Delta(p_i) = (p_i^{q^{-1}-1} - p_i^{q-1})/(q^{-1} - q)$. All of these entropies generalize the Shannon entropy and are nonextensive in the sense that $\mathcal{S}_q(A + B) = \mathcal{S}_q(A) + \mathcal{S}_q(B) + (1 - q)\mathcal{S}_q(A)\mathcal{S}_q(B)$. An additional level of generalization may be obtained if these entropies are computed in other domains such as the Fourier or the wavelet domains. The wavelet Tsallis q-entropy was studied in [32, 43], and this paper proposed the shifted wavelet (q, q')-entropy and studied their properties for fractal signal analysis. The (q, q') entropy was first proposed in [41], and for a given probability distribution $\{p_i\}_{i=1,2,3,\ldots N}$, is computed as follows:

$$\mathcal{S}_{(q,q')}(p_i) = -\sum_{i=1}^{N} \frac{(p_i)^q - (p_i)^{q'}}{q - q'}. \tag{2.9}$$

It has a $q \leftrightarrow q'$ invariance and is nonextensive. It is related with the Tsallis entropy according to the following:

$$\mathcal{S}_{(q,q')}(p_i) = \frac{(q-1)\mathcal{S}_q^T(p_i) - (q' - 1)\mathcal{S}_{q'}^T(p_i)}{q - q'}, \tag{2.10}$$

where $\mathcal{S}_q^T$ represents the Tsallis entropy of parameter q. A time-scale or wavelet (q, q')-entropy is obtained by substituting the RWE given by;

$$\mathrm{RWE}_{1/f} = 2^{(j-1)\alpha} \frac{1 - 2^{\alpha}}{1 - 2^{\alpha N}}, \tag{2.11}$$

to the equation given in Eq (2.9). Eq (2.9) represents the unnormalized (q, q')-entropy functional. However, for the purposes of the paper, a normalized version is used instead. Thus the normalized (q, q')-entropy functional is given by the following relation:

$$\begin{aligned} \mathcal{S}_{(q,q')}(p_i) &= \sum_i \frac{p_i^q - p_i^{q'}}{N^{1-q} - N^{1-q'}} \\ &= \mathcal{S}_q^T(p_i) \frac{1 - N^{1-q}}{N^{1-q} - N^{1-q'}} - \mathcal{S}_{q'}^T(p_i) \frac{1 - N^{1-q'}}{N^{1-q} - N^{1-q'}}. \end{aligned} \tag{2.12}$$

Therefore, the normalized wavelet (q, q')-entropy for fractal signals is obtained by substituting Eq (2.11) into Eq (2.12) to obtain the following:

$$\mathcal{S}_{(q,q')}(p_i) = \mathcal{S}_q^T(p_i) \frac{1 - N^{1-q}}{N^{1-q} - N^{1-q'}} - \mathcal{S}_{q'}^T(p_i) \frac{1 - N^{1-q'}}{N^{1-q} - N^{1-q'}}, \tag{2.13}$$

where $\mathcal{S}_q^T(p_i)$ is the wavelet Tsallis q-entropy given by the following relation:

$$\mathcal{S}_{(q)}^T(p_i) = \left\{ \frac{\mathrm{P}^{N-1}\left(2\cosh(\frac{\alpha q' \ln 2}{2})\right)}{\left(\mathrm{P}^{N-1}\left(2\cosh(\frac{\alpha \ln 2}{2})\right)\right)^{q'}} - \frac{\mathrm{P}^{N-1}\left(2\cosh(\frac{\alpha q \ln 2}{2})\right)}{\left(\mathrm{P}^{N-1}\left(2\cosh(\frac{\alpha \ln 2}{2})\right)\right)^{q}} \right\} \times K, \tag{2.14}$$

where $K = \left(N^{1-q} - N^{1-q'}\right)^{-1}$ and $\mathrm{P}^{N-1}(2\cosh u)$ is a polynomial of order $N-1$ of the following form:

$$\begin{aligned} P^{N-1}(.) = (2\cosh u)^{N-1} - \frac{(N-2)}{1!}(2\cosh u)^{N-3} \\ + \frac{(N-3)(N-4)}{2!}(2\cosh u)^{N-5} - \ldots \end{aligned} \tag{2.15}$$

Equation (2.13) is the wavelet (q, q')-entropy of fractal signals of parameter α and their properties are briefly described in [44].

3. Results and discussion

3.1. The shifted wavelet (q, q')-entropy

The RWE (Eq (2.11)) was computed using the wavelet spectrum (Eq (2.7)) substituted in the following:

$$\mathcal{E}_j = \frac{1}{N_j}\sum_k \mathbb{E}d_X^2(j,k),\ (j = 1, 2 \ldots \log_2(N)), \tag{3.1}$$

and averaged in all scales as in the following equation:

$$\mathrm{RWE}_j = \frac{\mathcal{E}_j}{\sum_j \mathcal{E}_j},\ (j = 1, 2 \ldots \log_2(N)), \tag{3.2}$$

where $N_j = 2^j$ is the number of wavelet coefficients at scale j. Additionally, Zunino and co-workers [40] introduced the unnormalized wavelet energy, which is computed using the following relation:

$$\mathcal{E}_j^U = \sum_k \mathbb{E}d_X^2(j,k)\ (j = 1, 2 \ldots \log_2(N)). \tag{3.3}$$

The unnormalized wavelet energy produces an unnormalized RWE, which is given by the following:

$$\mathrm{RWE}_{1/f}^U = 2^{(j-1)(\alpha-1)}\frac{1-2^{(\alpha-1)}}{1-2^{(\alpha-1)N}}, \tag{3.4}$$

and which is a version of the RWE shifted by 1 (in the fractality index range). Motivated by this, it is therefore evident that by computing the wavelet energy in the following form:

$$\mathcal{E}_j^W = (N_j)^r \times \sum_k \mathbb{E}d_X^2(j,k). \tag{3.5}$$

The following weighted RWE is obtained:

$$\mathrm{wRWE}_{1/f} = 2^{(j-1)(\alpha-r)}\frac{1-2^{(\alpha-r)}}{1-2^{(\alpha-r)N}}, \tag{3.6}$$

Equation (3.6) is a shifted by the r (in the fractality range) version of the standard RWE given in Eq (2.11). Therefore, the weighted RWE (wRWE) is a more general probability mass function (pmf) to compute entropies in fractal signals and permits obtaining novel versions of the wavelet entropies presented earlier in the literature.

Theorem 3.1. *Let $p_i = wRWE_{1/f}$ be the shifted by r RWE of fractal signals and $\mathcal{S}_{(q,q')}(.)$ be the normalized $(q, q')-$entropy functional. Then,*

$$\mathcal{S}_{(q,q')}(wRWE_{1/f}) = \mathcal{S}^T_{(q,r)}(p_i)\frac{1-N^{1-q}}{N^{1-q}-N^{1-q'}} - \mathcal{S}^T_{(q',r)}(p_i)\frac{1-N^{1-q'}}{N^{1-q}-N^{1-q'}}, \tag{3.7}$$

where $\mathcal{S}^T_{(q,r)}(p_i)$ and $\mathcal{S}^T_{(q',r)}(p_i)$ are the shifted wavelet Tsallis entropies of parameter q and shift r and parameter q' and shift r, respectively.

Proof. Recall from Eq (2.12) that

$$\mathcal{S}_{(q,q')}(p_i) = \mathcal{S}^T_q(p_i)\frac{1-N^{1-q}}{N^{1-q}-N^{1-q'}} - \mathcal{S}^T_{q'}(p_i)\frac{1-N^{1-q'}}{N^{1-q}-N^{1-q'}};$$

therefore, by computing $\mathcal{S}^T_q(p_i)$, using $p_i = \mathrm{wRWE}_{1/f}$, the following is obtained:

$$\begin{aligned}\mathcal{S}^T_q(\mathrm{wRWE}_{1/f}) &= \frac{1}{1-N^{1-q}}\left\{1-\sum_{i=1}^{N}\left(2^{(j-1)(\alpha-r)}\frac{1-2^{\alpha-r}}{1-2^{(\alpha-r)N}}\right)^q\right\}\\ &= \frac{1}{1-N^{1-q}}\left\{1-\left(\frac{1-2^{(\alpha-r)}}{1-2^{(\alpha-r)N}}\right)^q\left(\frac{1-2^{(\alpha-r)qN}}{1-2^{(\alpha-r)q}}\right)\right\}\\ &= \mathcal{S}^T_{(q,r)}(\mathrm{RWE}_{1/f}).\end{aligned}$$

Using a similar approach,

$$\mathcal{S}^T_{q'}(\mathrm{wRWE}_{1/f}) = \mathcal{S}^T_{(q',r)}(\mathrm{RWE}_{1/f}) :$$

therefore, substituting $\mathcal{S}^T_{(q,r)}(\mathrm{wRWE}_{1/f})$ and $\mathcal{S}^T_{(q',r)}(\mathrm{wRWE}_{1/f})$, Eq (3.7) results.

Moreover, a shifted version of the wavelet Shannon entropy presented in Zunino [40], computed in the same way as the shifted Tsallis is given by the following:

$$\mathrm{H}_{\alpha-r} = \frac{1}{\log_2(N)}\left\{\left[\frac{(\alpha-r)N}{1-2^{-(\alpha-r)N}} + \frac{\alpha-r}{1-2^{-(\alpha-r)}}\right] - \log_2\left(\frac{1-2^{(\alpha-r)}}{1-2^{(\alpha-r)N}}\right)\right\}. \tag{3.8}$$

Therefore, the shifted wavelet (q, q')-entropy is given by the following relation:

$$\mathcal{S}^r_q(p_i) = \mathcal{S}^T_{(q,r)}(p_i)\frac{1-N^{1-q}}{N^{1-q}-N^{1-q'}} - \mathcal{S}^T_{(q',r)}(p_i)\frac{1-N^{1-q'}}{N^{1-q}-N^{1-q'}},$$

where $\mathcal{S}^T_{(q,r)}(p_i)$ is the shifted wavelet Tsallis entropy of parameter q and shift r, which is given by the following:

$$\mathcal{S}^T_{(q,r)}(p_i) = \left\{\frac{\mathrm{P}^{N-1}\left(2\cosh(\frac{(\alpha-r)q'\ln 2}{2})\right)}{\left(\mathrm{P}^{N-1}\left(2\cosh(\frac{(\alpha-r)\ln 2}{2})\right)\right)^{q'}} - \frac{\mathrm{P}^{N-1}\left(2\cosh(\frac{(\alpha-r)q\ln 2}{2})\right)}{\left(\mathrm{P}^{N-1}\left(2\cosh(\frac{(\alpha-r)\ln 2}{2})\right)\right)^{q}}\right\} \times K, \tag{3.9}$$

where

$$K = \left(N^{1-q} - N^{1-q'}\right)^{-1}$$

and the polynomial given in Eq (3.9), $\mathrm{P}^{N-1}(u)$, is obtained as follows:

$$\begin{aligned} P^{N-1}(.) = (2\cosh u)^{N-1} - \frac{(N-2)}{1!}(2\cosh u)^{N-3} \\ + \frac{(N-3)(N-4)}{2!}(2\cosh u)^{N-5} - \ldots \end{aligned} \tag{3.10}$$

Therefore, the shifted wavelet (q, q')-entropy is an entropy with the same characteristics and advantages as the standard wavelet (q, q')-entropy; however, unlike the standard version, the shifted version provides an extra parameter r, which allows us to shift the wavelet (q, q') entropy values to any point of the scaling index range, thus increasing the analysis flexibility of the fractals.

3.2. Properties and applications of the shifted wavelet (q, q')*-entropy*

As mentioned above, the shifted wavelet (q, q')-entropy has similar properties and information planes as those of their standard version but shifted at $\alpha = r$. This means that it is maximal at $\alpha = r$ (or around r), increasing for $\alpha < r$ and decreasing for $\alpha > r$. In addition, the shape or their information planes is controlled by parameters q and q'; based on these, the shifted wavelet Shannon and Tsallis entropies may be obtained when $(q, q') \to (1, 1)$ and $q' \to 1$, respectively. In the following, shifted wavelet (q, q') entropy planes are obtained and discussed for fractal signals of parameter α.

3.3. Shifted wavelet (q, q') *information planes*

Figure 1 shows the shifted wavelet (q, q')-entropy planes for two different values of the pair (q, q'), $r = 0$, $\log_2(N) \in [5, 15]$ and the fractality parameter $-4 < \alpha < 4$ along with three 2D slices corresponding to signal lengths $\log_2(N) = 7, 9, 11$. The top left plot presents the $(q, q') \to (0.9, 1)$ case. From this plot note that the entropies are maximal at $\alpha = 0$, increasing for $\alpha < 0$, decreasing for $\alpha > 0$, and symmetrical at the origin ($\alpha = 0$). The bottom left plot shows three different 2D slices of the shifted wavelet plane of the top left plots that highlight the signal length effect on the entropy values. From this plot note that the entropic values are slightly affected by signal length. The top right plot shows the shifted wavelet entropy planes for $q = 12$, $q' = 1$, $r = 0$, $\log_2(N) \in [5, 15]$, and $-4 < \alpha < 4$. As in the previous case, the entropies are increasing for $\alpha < 0$, decreasing for $\alpha > 0$, and symmetrical at $\alpha = 0$; however, they are maximal in an interval of the fractality range $(-\alpha_C/2 < \alpha < \alpha_C/2)$, and the length of this interval can be controlled by q (or q'). In addition, the 2D slices for $\log_2(N) = 7, 9, 11$ in the bottom right plot reveals that signal length is irrelevant for $q \gg 1$.

As mentioned earlier, when $r \neq 0$, the wavelet entropy values are either shifted or relocated at $\alpha = r$. This means that for identical q, q', and N, the shape of the wavelet entropies are identical but located in different regions of the fractality parameter α. For $r \neq 0$, the shifted wavelet entropies are symmetrical at $\alpha = r$, increasing for $\alpha < r$, and decreasing for $\alpha > r$. Figure 2 illustrates the entropies when $r = 0, 2, 4, 6$ and the parameters q, q', and N identical. Note that the shape of the entropies are identical though the location is affected by the value of r. This means that the entropies are symmetrical around r, decreasing for $\alpha > r$, and increasing for $\alpha < r$. In addition, when $q \gg 1$ and $q' \to 1$, constant regions of maximum entropies are observed in the interval $r - \alpha_C/2 < \alpha < r + \alpha_C/2$. This means that constant entropies are observed for $|\alpha - r| < \alpha_C/2$ and varying for $|\alpha - r| > \alpha_C/2$. This result is of a significant importance since a given fractal signal family can be mapped to $|\alpha - r| > \alpha_C/2$ and can discriminate these fractals by means of constant/nonconstant entropies. For instance, if $r + \alpha_C = 0$,

then the discrimination between long-memory and short-memory signals may be achieved, and when $r + \alpha_C = 1$, stationarity versus nonstationarity can be discriminated. In addition, within a fractal signal, a specific behavior may be of interest such as the strong correlations versus weak correlations in long-memory signals.

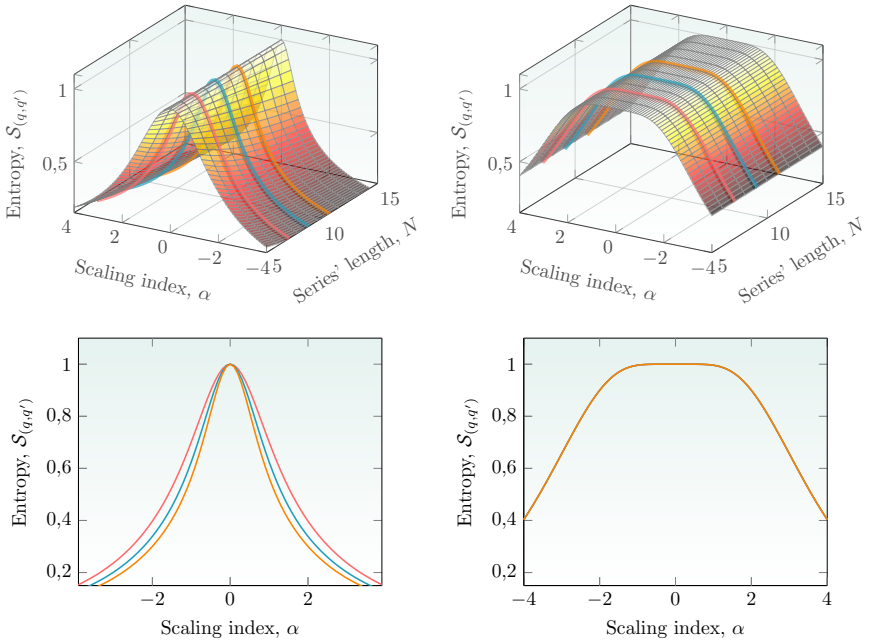

Figure 1. Shifted wavelet (q, q')-entropy planes for $r = 0$, $5 \leq N \leq 15$ and $\alpha \in [-4, 4]$. The top left plot shows the case $(q, q') \to (0.9, 1)$ along with lines representing the signal length $N = 7, 9, 11$. The bottom left plot shows the effect of the signal length of the top left plot for $N = 7, 9, 11$. The top right plot shows the $(q, q') \to (12, 1)$ case and the bottom right plot the dependence of the top right case to the signal length.

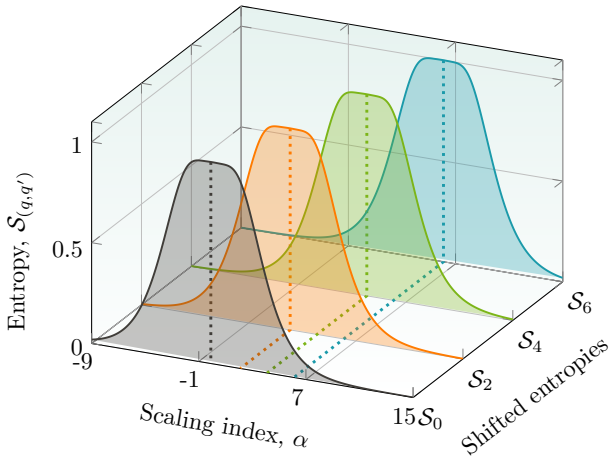

Figure 2. Shifted wavelet (q, q')-entropies for different values of r. $\mathcal{S}_0$ corresponds to the standard wavelet (q, q')-entropy ($r = 0$), $\mathcal{S}_2$ is a shifted by the $r = 2$ wavelet entropy, $\mathcal{S}_2$ for $r = 4$, and $\mathcal{S}_6$ for $r = 6$.

4. Classification of long-memory and short-memory signals

An important family of fractal signals is the class of stationary fractal process ($0 < \alpha < 1$), which can be further categorized as short-memory fractals ($0 < \alpha < 1/2$) and long-memory fractals ($1/2 < \alpha < 1$). The fractality point $\alpha = 1/2$ is the limit between the short-memory and long-memory behavior and permits the discrimination between those two processes: For $\alpha > 1/2$, the signals are long-memory and for $\alpha < 1/2$, the signals are short-memory. Therefore, by using the shifted wavelet (q, q')-entropy with $q \gg 1$ and $r + \alpha_C = 1/2$, the discrimination between these two signals may be achieved by the principle that one family will experiment constant entropies while the other varyies. The left plot of Figure 3 displays the results of this classification for fGn noise signals with length $N = 8192$ which is generated by the Paxson FFT method. For the classifcation, 100 fGn signals in the range $(1 + \alpha)/2 = H \in \{0.01, .02, \ldots, 0.94, 0.95\}$ were generated. This means that 9500 fGn series in total were employed for the classification. The shifted wavelet entropies were estimated within a signal in blocks, using sliding windows; therefore, for every signal, $\{\mathcal{S}_{(q,r)}(i), i = 1, 2, \ldots\}$ entropies were obtained. Finally, a variability measure was applied to these entropies by means of the biweigth midvariance. As can be seen in the figure, the shifted wavelet entropies not only allow us to classify SRD and LRD signals, but also to perform it efficiently since no other signal is classified as LRD after a certain point within H. Additionally, the plot includes a reference line to indicate the limit $H = 0.5$.

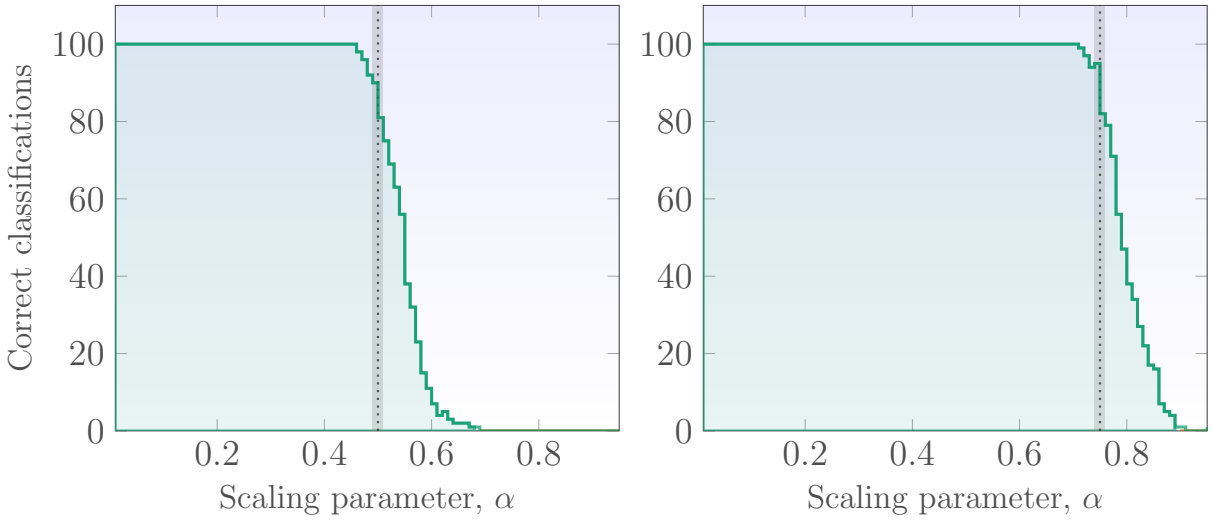

Figure 3. Classification results for stationary fractal signals. The left plot shows the results for SRD versus LRD and the right plot shows an example for a classification within the LRD (processes which are less than $H = 0.75$) and processes which have a higher H.

Here, it is important to note, that although some methodologies exist which classify the LRD and SRD processes, no other tools has been proposed to classify LRD as "strong" LRD and "light" LRD signals. By light and strong, we refer to LRD processes with $H < 0.75$ and $H > 0.75$, respectively. The right plot of Figure 3 displays this classification by modifying r accordingly. The classification was performed in a similar manner as for $H = 0.5$, with respect to sliding windows and with the use of the biweigth midvariance. Note, the classifications are also well performed, thereby quickly

decaying to 0 for $H > 0.75$. Additionally any other classification within the stationary limit of α may be perfomed; therefore, the shifted wavelet (q, q')-entropy allows us to efficiently classify the stationary fractal signals by modifying the RWE of the process.

5. Conclusions

In this contribution, a shifted version of the wavelet (q, q')-entropy was presented. The shifted wavelet entropy allowed us to shift the characteristics of the original wavelet (q, q')-entropy by computing it on a weighted RWE. It was shown that there is a direct relationship between the weight of the RWE and the shift of the wavelet (q, q')-entropy. The shifted wavelet entropy information planes were obtained and based on these, potential applications were highlighted. An example application focused on the classification of stationary fractal signals and it was shown that the shifted wavelet (q, q') allows us to not only efficiently classify LRD versus SRD fractals and light versus strong LRD fractal signals, but also any other signals within the stationary fractal signal range.

Author contributions

Julio César Ramírez Pacheco and Luis Rizo-Dpmínguez conceived the idea, Joel Antonio Trejo-Sáncez designed the methodology and the main proof. All authors contributed equally in the writing of the article.

Use of AI tools declaration

The authors declare they have not used Artificial Intelligence (AI) tools in the creation of this article.

Acknowledgments

Julio César Ramírez Pacheco thanks the suppport for Autonomous University of Quintana Roo and also the suppor offered by The Science, Engineering and Technology Division at UQRoo.

Conflict of interest

The authors declare there is no conflict of interest.

References

1. B. B. Mandelbrot, J. R. Wallis, Noah, joseph, and operational hydrology, *Water Resour. Res.*, **4** (1968), 909–918. https://doi.org/10.1029/WR004i005p00909
2. G. G. Booth, F. R. Kaen, P. E. Koveos, R/S analysis of foreign exchange rates under two international monetary regimes, *J. Monet. Econ.*, **10** (1982), 407–415. https://doi.org/10.1016/0304-3932(82)90035-6
3. P. Gilfriche, V. Deschodt-Arsac, E. Blons, L. M. Arsac, Frequency-specific fractal analysis of postural control accounts for control strategies, *Front. Physiol.*, **9** (2018), 293. https://doi.org/10.3389/fphys.2018.00293

4. M. Frezza, A fractal-based approach for modeling stock price variations, *Chaos*, **28** (2018), 091102. https://doi.org/10.1063/1.5050867
5. L. P. Bu, P. J. Shang, Scaling analysis of stock markets, *Chaos*, **24** (2014), 023107. https://doi.org/10.1063/1.4871479
6. C. Y. Zhang, H. Y. Cui, Z. Z. He, L. Su, D. Fu, Fractals in carbon nanotube buckypapers, *RSC Adv.*, **6** (2016), 8639–8643. https://doi.org/10.1039/C5RA23465D
7. M. A. Fernandes, E. A. Ribeiro Rosa, A. Cristina, A. M. T. Grégio, P. C. Trevilatto, L. R. Azevedo-Alanis, Applicability of fractal dimension analysis in dental radiographs for the evaluation of renal osteodystrophy, *Fractals*, **24** (2016), 1650010. https://doi.org/10.1142/S0218348X16500109
8. S. W. Ducharme, R. E. A. van Emmerik, Fractal dynamics, variability, and coordination in human locomotion, *Kinesiology Rev.*, **7** (2018), 26–35. https://doi.org/10.1123/kr.2017-0054
9. J. Sen, D. McGill, Fractal analysis of heart rate variability as a predictor of mortality: A systematic review and meta-analysis, *Chaos*, **28** (2018), 072101. https://doi.org/10.1063/1.5038818
10. A. L. Goldberger, L. A. Amaral, J. M. Hausdorff, P. C. Ivanov, C. K. Peng, H. E. Stanley, Fractal dynamics in physiology: Alterations with disease and aging, *Proc. Nat. Acad. Sci.*, **99** (2002), 2466–2472. https://doi.org/10.1073/pnas.012579499
11. D. G. Stephen, J. Anastas, Fractal fluctuations in gaze speed visual search, *Atten. Percept. Psychophys*, **73** (2011), 666–677. https://doi.org/10.3758/s13414-010-0069-3
12. M. Iosa, G. Morone, A. Fusco, F. Marchetti, C. Caltagirone, S. Paolucci, et al., Loss of fractal gait harmony in Parkinson's Disease, *Clin. Neurophysiol.*, **127** (2016), 1540–1546. https://doi.org/10.1016/j.clinph.2015.11.016
13. L. G. A. Alves, P. B. Winter, L. N. Ferreira, R. M. Brielmann, R. I. Morimoto, L. A. N. Amaral, Long-range correlations and fractal dynamics in c. elegans: Changes with aging and stress, *Phys. Rev. E*, **96** (2017), 022417. https://doi.org/10.1103/PhysRevE.96.022417
14. P. Li, L. Yu, A. S. P. Lim, A. S. Buchman, F. A. J. L. Scheer, S. A. Shea, et al., Fractal regulation and incident alzheimer's disease in elderly individuals, *Alzheimers. Dement.*, **14** (2018), 1114–1125. https://doi.org/10.1016/j.jalz.2018.03.010
15. M. Gilmore, C. X. Yu, T. L. Rhodes, W. A. Peebles, Investigation of rescaled range analysis, the hurst exponent, and long-time correlations in plasma turbulence, *Phys. Plasmas*, **9** (2002), 1312–1317. https://doi.org/10.1063/1.1459707
16. P. Xu, A discussion on fractal models for transport physics of porous media, *Fractals*, **23** (2015), 1530001. https://doi.org/10.1142/S0218348X15300019
17. J. Beran, R. Sherman, M. S. Taqqu, W. Willinger, Long-range dependence in variable-bit-rate video traffic, *IEEE Trans. Commun.*, **43** (1995), 1566–1579. https://doi.org/10.1109/26.380206
18. F. Serinaldi, Use and misuse of some hurst parameter estimators applied to stationary and non-stationary financial time series, *Physica A*, **389** (2010), 2770–2781. https://doi.org/10.1016/j.physa.2010.02.044
19. P. Abry, D. Veitch, Wavelet analysis of long-range-dependent traffic, *IEEE Trans. Inf. Theory*, **44** (1998), 2–15. https://doi.org/10.1109/18.650984

20. S. Stoev, M. S. Taqqu, C. Park, J. S. Marron, On the wavelet spectrum diagnostic for hurst parameter estimation in the analysis of internet traffic, *Comput. Netw.*, **48** (2005), 423–445. https://doi.org/10.1016/j.comnet.2004.11.017

21. C. K. Peng, S. V. Buldyrev, S. Havlin, M. Simons, H. E. Stanley, A. L. Goldberger, Mosaic organization of dna nucleotides, *Phys. Rev E*, **49** (1994), 1685. https://doi.org/10.1103/PhysRevE.49.1685

22. P. Ferreira, What detrended fluctuation analysis can tell us about nba results, *Physica A*, **500** (2018), 92–96. https://doi.org/10.1016/j.physa.2018.02.050

23. J. Kwapień, P. Oświecimka, S. Drożdż, Detrended fluctuation analysis made flexible to detect range of cross-correlated fluctuations, *Phys. Rev. E*, **92** (2015), 052815. https://doi.org/10.1103/PhysRevE.92.052815

24. T. K. Lin, H. Fajri, Damage detection of structures with detrended fluctuation and detrended cross-correlation analyses, *Smart Mater. Struct.*, **26** (2017), 035027. https://doi.org/10.1088/1361-665X/aa59d7

25. J. C. Gallant, I. D. Moore, M. F. Hutchinson, P. Gessler, Estimating fractal dimension of profiles: A comparison of methods, *Math. Geol.*, **26** (1994), 455–481. https://doi.org/10.1007/BF02083489

26. B. Pilgram, D. T. Kaplan, A comparison of estimators for 1f noise, *Physica D*, **114** (1998), 108–122. https://doi.org/10.1016/S0167-2789(97)00188-7

27. T. Stadnitski, Measuring fractality, *Front. Physiol.*, **3** (2012), 127. https://doi.org/10.3389/fphys.2012.00127

28. M. S. Taqqu, V. Teverovsky, W. Willinger, Estimators for long-range dependence: An empirical study, *Fractals*, **3** (1995), 785–798. https://doi.org/10.1142/S0218348X95000692

29. A. Eke, P. Herman, L. Kocsis, L. R. Kozak, Fractal characterization of complexity in temporal physiological signals, *Physiol. Meas.*, **23** (2002), R1. https://doi.org/10.1088/0967-3334/23/1/201

30. A. Eke, P. Herman, J. Bassingthwaighte, G. Raymond, D. Percival, M. Cannon, et al., Physiological time series: Distinguishing fractal noises from motions, *Pflügers Arch. Eur. J. Physiol.*, **439** (2000), 403–415. https://doi.org/10.1007/s004249900135

31. D. Delignieres, S. Ramdani, L. Lemoine, K. Torre, M. Fortes, G. Ninot, Fractal analyses for 'short'time series: A re-assessment of classical methods, *J. Math. Psychol.*, **50** (2006), 525–544. https://doi.org/10.1016/j.jmp.2006.07.004

32. J. Ramirez Pacheco, D. Torres Román, H. Toral Cruz, Distinguishing stationary/nonstationary scaling processes using wavelet tsallis-entropies, *Math. Probl. Eng.*, **2012** (2012), 867042. https://doi.org/10.1155/2012/867042

33. O. Nicolis, J. Mateu, J. E. Contreras-Reyes, Wavelet-based entropy measures to characterize two-dimensional fractional Brownian fields, *Entropy*, **22** (2020), 196. https://doi.org/10.3390/e22020196

34. C. Bandt, B. Pompe, Permutation entropy: A natural complexity measure for time series, *Phys. Rev. Lett.*, **88** (2002), 174102. https://doi.org/10.1103/PhysRevLett.88.174102

35. Y. H. Cao, W. Tung, J. B. Gao, V. A. Protopopescu, L. M. Hively, Detecting dynamical changes in time series using the permutation entropy, *Phys. Rev. E*, **70** (2004), 046217. https://doi.org/10.1103/PhysRevE.70.046217
36. C. Tsallis, Possible generalization of boltzmann-gibbs statistics, *J. Stat. Phys.*, **52** (1998), 479–487. https://doi.org/10.1007/BF01016429
37. P. A. Varotsos, N. V. Sarlis, H. K. Tanaka, E. S. Skordas, Some properties of the entropy in the natural time, *Phys. Rev. E*, **71** (2005), 032102. https://doi.org/10.1103/PhysRevE.71.032102
38. G. E. Powell, I. C. Percival. A spectral entropy method for distinguishing regular and irregular motion of hamiltonian systems, *J. Phys. A Math. Gen.*, **12** (1979), 2053. https://doi.org/10.1088/0305-4470/12/11/017
39. D. G. Perez, L. Zunino, M. Garavaglia, O. A. Rosso, Wavelet entropy and fractional brownian motion time series, *Physica A*, **365** (2006), 282–288. https://doi.org/10.1016/j.physa.2005.09.060
40. L. Zunino, D. G. Perez, M. Garavaglia, O. A. Rosso, Wavelet entropy of stochastic processes, *Physica A*, **379** (2007), 503–512. https://doi.org/10.1016/j.physa.2006.12.057
41. E. P. Borges, Itzhak Roditi, A family of nonextensive entropies, *Phys. Lett. A*, **246** (1998), 399–402. https://doi.org/10.1016/S0375-9601(98)00572-6
42. W. X. Ren, Z. S. Sun, Structural damage identification by using wavelet entropy, *Eng. Struct.*, **30** (2008), 2840–2849. https://doi.org/10.1016/j.engstruct.2008.03.013
43. J. Ramirez-Pacheco, D. Torres-Roman, Cosh window behaviour of wavelet tsallis q-entropies in 1/f α signals, *Electron. Lett.*, **47** (2011), 186–187. https://doi.org/10.1049/el.2010.7167
44. J. Ramírez-Pacheco, L. Rizo-Domínguez, J. A. Trejo-Sánchez, J. Cortez-González, A nonextensive wavelet (q, q')-entropy for $1/f^{\alpha}$ signals, *Rev. Mex. de Fis.*, **62** (2016), 229–234.
45. M. Maejima, On a class of self-similar processes, *Probab. Theory Relat. Fields*, **62** (1983), 235–245. https://doi.org/10.1007/BF00538799
46. B. D. Malamud, D. L. Turcotte, Self-affine time series: Measures of weak and strong persistence, *J. Stat. Plan. Inference*, **80** (1999), 173–196. https://doi.org/10.1016/S0378-3758(98)00249-3
47. J. E. Contreras-Reyes, Jensen-autocorrelation function for weakly stationary processes and applications, *Physica D*, **470** (2024), 134424. https://doi.org/10.1016/j.physd.2024.134424
48. J. Geweke, S. Porter-Hudak, The estimation and application of long memory time series models, *J. Time Ser. Anal.*, **4** (1983), 221–238. https://doi.org/10.1111/j.1467-9892.1983.tb00371.x
49. C. W. J. Granger, R. Joyeux, An introduction to long-memory time series models and fractional differencing, *J. Time Ser. Anal.*, **1** (1980), 15–29. https://doi.org/10.1111/j.1467-9892.1980.tb00297.x
50. D. B. Percival, Stochastic models and statistical analysis for clock noise, *Metrologia*, **40** (2003), S289. https://doi.org/10.1088/0026-1394/40/3/308
51. A. Cohen, J. Kovacevic, Wavelets: The mathematical background, *Proc. IEEE*, **84** (1996), 514–522. https://doi.org/10.1109/5.488697
52. L. Hudgins, C. A. Friehe, M. E. Mayer, Wavelet transforms and atmopsheric turbulence, *Phys. Rev. Lett.*, **71** (1993), 3279. https://doi.org/10.1103/PhysRevLett.71.3279

53. P. Abry, P. Gonçalvés, P. Flandrin, Wavelets, spectrum analysis and 1/f processes, In: *Wavelets and Statistics*, New York: Springer, 1995, 15–29. https://doi.org/10.1007/978-1-4612-2544-7-2

54. G. W. Wornell, A. V. Oppenheim, Estimation of fractal signals from noisy measurements using wavelets, *IEEE Trans. Signal Process.*, **40** (1992), 611–623. https://doi.org/10.1109/78.120804

55. S. G. Mallat, A theory for multiresolution signal decomposition: The wavelet representation, in *IEEE Transactions on Pattern Analysis and Machine Intelligence*, IEEE, **11** (1989), 674–693. https://doi.org/10.1109/34.192463

56. P. Abry, D. Veitch, P. Flandrin, Long-range dependence: Revisiting aggregation with wavelets, *J. Time Ser. Anal.*, **19** (1998), 253–266. https://doi.org/10.1111/1467-9892.00090

57. L. Eduardo Virgilio Silva, L. Otavio Murta Jr, Evaluation of physiologic complexity in time series using generalized sample entropy and surrogate data analysis, *Chaos*, **22** (2012), 043105. https://doi.org/10.1063/1.4758815

58. M. J. Xu, P. J. Shang, J. J. Huang, Modified generalized sample entropy and surrogate data analysis for stock markets, *Commun. Nonlinear Sci. Numer. Simul.*, **35** (2016), 17–24. https://doi.org/10.1016/j.cnsns.2015.10.023

59. G. Kaniadakis, M. Lissia, A. M. Scarfone, Two-parameter deformations of logarithm, exponential, and entropy: A consistent framework for generalized statistical mechanics, *Phys. Rev. E*, **71** (2005), 046128. https://doi.org/10.1103/PhysRevE.71.046128

60. G. Kaniadakis, Statistical mechanics in the context of special relativity, *Phys. Rev. E*, **66** (2002), 056125. https://doi.org/10.1103/PhysRevE.66.056125

61. S. Abe, A note on the q-deformation-theoretic aspect of the generalized entropies in nonextensive physics, *Phys. Lett. A*, **224** (1997), 326–330. https://doi.org/10.1016/S0375-9601(96)00832-8

AIMS Press